ISSN 0208-7774 TRIBOLOGIA 4/2018 p. 49–54

Marek MARTYNA*, Jan ZWOLAK**

ANALYSIS INTO THE INFLUENCE OF SELECTED TOOTHED GEAR PARAMETERS ON THE VALUE OF SLIPPAGE AND CONTACT STRESSES IN A CYLINDRICAL GEARBOX

ANALIZA WPŁYWU WYBRANYCH PARAMETRÓW KÓŁ ZĘBATYCH NA WARTOŚĆ POŚLIZGU MIĘDZYZĘBNEGO I NAPRĘŻEŃ KONTAKTOWYCH W PRZEKŁADNI ZĘBATEJ WALCOWEJ

Key words: toothed gears, contact stress, slippage, multi-criterion optimization.

Abstract The paper presents issues concerning the geometrical and durability calculations of power shift gearboxes with multi-criterion optimization, using proprietary computer software. Among many parameters influencing the value of slippage and contact stresses, the flank ratio at P-0 correction and P correction, the value of the flank angle, and the module value were analysed. The slippage was analysed at Point B_1, which belongs to the beginning of the single tooth engagement area, as well as in Point B_2, where the single tooth engagement area ends. Contact stresses were calculated at Point C, which is the pitch point. Their values were referenced to experimentally determined fatigue contact durability σ_{Hlim}.

Słowa kluczowe: koła zębate, naprężenia kontaktowe, poślizg międzyzębny, optymalizacja wielokryterialna.

Streszczenie W pracy przedstawiono zagadnienia dotyczące obliczeń geometrycznych i wytrzymałościowych przekładni zębatych power shift, z optymalizacją wielokryterialną, przy stosowaniu autorskiego programu komputerowego. Wśród wielu parametrów mających wpływ na wartość poślizgu międzyzębnego i naprężeń kontaktowych analizowano współczynnik przesunięcia zarysu przy korekcji P-0 i korekcji P, wartość kąta zarysu i wartość modułu. Poślizgi analizowano w punkcie B_1 należącym do początku strefy jednoparowego zazębienia oraz w punkcie B_2, w którym kończy się strefa jednoparowego zazębienia. Naprężenia kontaktowe obliczano w punkcie C będącym biegunem zazębienia, a ich wartości odnoszono do wyznaczonej doświadczalnie zmęczeniowej wytrzymałości kontaktowej σ_{Hlim}.

INTRODUCTION

In the structure of power transmission systems of mobile engineering machines, there is a power shift gearbox **[L. 1, 3, 4]**, which a characteristic feature being that the toothed gears remain in continuous engagement with each other. A change of gear ratio takes place through multidisc friction clutches (the so-called wet clutches), integrated with toothed gears mounted on a common shaft. These clutches consist of an appropriate number of friction and steel discs (depending on the transmitted torque). Friction discs have an internal spline connecting them to the toothed gear, while steel discs have an external spline that connects them to the shaft via a clutch basket. The clutch basket constitutes a permanent spline connection with the shaft, independent of the toothed gear. In the event that there is clearance between the friction discs and steel discs (there is no pressure), the clutch does not transfer the torque from the shaft to the toothed gears. The clutch switches on when the friction coupling between the friction discs and the steel discs occurs as a result of pressing them against each other through a hydraulic cylinder, which is an integral part of the clutch.

Contact stresses and slippage on individual gear ratios differ from each other quite significantly. It is possible to reduce these differences by the appropriate selection of the toothed gear's design parameters, which

* Liugong Dressta Machinery, ul. Kwiatkowskiego 1, 37-450 Stalowa Wola, Poland, tel. 15 8136284.
** University of Rzeszów, al. Rejtana 16c, 35-959 Rzeszów, Poland, tel. 17 8518582.

can be obtained by multi-criterion optimization. In the gearbox under consideration, there are toothed gears in which engagement frequency (i.e. with how many toothed gears a given gear forms a toothed pair) equals one, two, and three at the largest. For example, a tooth engagement equal to one is typical of toothed gear z_1, which forms a toothed pair only with the z_3 gear (**Figs. 1** and **2**). Tooth engagement equal to two is assigned to gear z_8, forming a toothed pair with gear z_6 and gear z_{11}. The largest tooth engagement in the gearbox equalling three has the toothed gear z_3, which engages with gears: z_1, z_5, and z_{10}. An example of a toothed pair that forms a circle with gears, z_1, z_5, z_{10}, is presented in **Figure 1**.

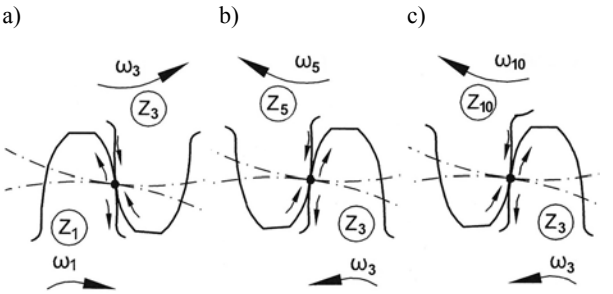

Fig. 1. Toothed pairs with slip vectors: a) z_3:z_1, b) z_3:z_5, c) z_3:z_{10}

Rys. 1. Pary zębate z wektorami poślizgu: a) z_3:z_1, b) z_3:z_5, c) z_3:z_{10}

The presented engagement frequency shows that, at the specified time of gearbox operation, the toothed gear z_3 will be subjected to the largest number of load cycles, which means that, on the active surface of the gear, it is most likely to experience surface wear by pitting. In the real gearbox within the toothed pair z_3:z_1 (**Fig. 1a**), the driver gear is the gear z_1, in which the slippage vectors are directed from the pitch point towards the head and root of the tooth. On the other hand, the z_3 gear is the follower gear with slippage directed towards the pitch point. In gear z_1 during operation, one side of the tooth remains in continuous contact with tooth of the gear z_3. In the toothed pair z_3:z_5 (**Fig. 1b**) and in the toothed pair z_3:z_{10} (**Fig. 1c**), the driver gear is the gear z_3, and the gears z_5 and z_{10} are follower gears. Thus, in gear z_3, one of the side surfaces of the teeth experiences a load from gears z_5 and z_{10}, and the other side from gear z_1. At designing and constructing stages, the designer should aim to minimize the slippage, while making sure that the contact durability σ_{Hlim} is fully utilized. The original computer software **[L. 7, 15]** uses values of fatigue contact durability σ_{Hlim} and fatigue durability of the tooth root σ_{Flim}, determined experimentally **[L. 8]** on a test bench within a circulating power system for five steel grades and two finishing technologies of the gears under investigation.

SUBJECT OF STUDY

The subject of numerical research in the area slippage and contact stresses was the power shift gearbox, whose kinematic scheme in axial and radial sections are shown in **Figure 2**.

The tested gearbox has 8 gear ratios (4 forward and 4 reverse). Its main components are 14 toothed gears, 7 shafts and 6 multidisc clutches. Clutches P and W on shaft I are integrated with toothed gears z_1 and z_2, which are responsible for forward and reverse motion, respectively. The S_1 and S_3 clutches are integrated with toothed gears z_7 and z_8 and allow connecting these wheels to shaft III. Subsequent clutches S_2 and S_4 integrated with gears z_{11} and z_{12} connect the gears with the IV shaft. The z_8 and z_9 toothed gears constitute a fixed connection with shaft V through a spline. The toothed gear z_{13} also constitutes a fixed spline connection with the output shaft VI. The toothed gear z_{14} on shaft VII plays the role of an intermediate gear in the kinematic chain of ratios i_5 to i_8 during reverse motion. Clutches S_1 to S_4 are responsible for implementing gears in the full range from i_1 to i_8 being under load of any toothed pair.

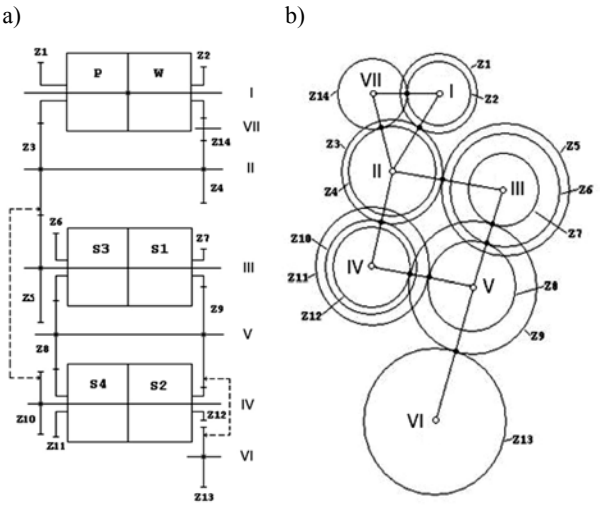

Fig. 2. Kinematic scheme of the power shift gearbox: a) axial alignment, b) radial alignment

Rys. 2. Schemat kinematyczny przekładni zębatej power shift: a) układ osiowy, b) układ promieniowy

Using **Figure 2**, kinematic chains from relevant toothed pairs will be created, starting from the input shaft I to the output shaft VI, for individual gear ratios.

$$i_1 = \frac{z_3}{z_1} \cdot \frac{z_5}{z_3} \cdot \frac{z_9}{z_7} \cdot \frac{z_{13}}{z_9}$$

$$i_2 = \frac{z_3}{z_1} \cdot \frac{z_{10}}{z_3} \cdot \frac{z_9}{z_{12}} \cdot \frac{z_{13}}{z_9}$$

$$i_3 = \frac{z_3}{z_1} \cdot \frac{z_5}{z_3} \cdot \frac{z_8}{z_6} \cdot \frac{z_{13}}{z_9}$$

$$i_4 = \frac{z_3}{z_1} \cdot \frac{z_{10}}{z_3} \cdot \frac{z_8}{z_{11}} \cdot \frac{z_{13}}{z_9}$$

$$i_5 = \frac{z_{14}}{z_2} \cdot \frac{z_4}{z_{14}} \cdot \frac{z_5}{z_3} \cdot \frac{z_9}{z_7} \cdot \frac{z_{13}}{z_9}$$

$$i_6 = \frac{z_{14}}{z_2} \cdot \frac{z_4}{z_{14}} \cdot \frac{z_{10}}{z_3} \cdot \frac{z_9}{z_{12}} \cdot \frac{z_{13}}{z_9}$$

$$i_7 = \frac{z_{14}}{z_2} \cdot \frac{z_4}{z_{14}} \cdot \frac{z_5}{z_3} \cdot \frac{z_8}{z_6} \cdot \frac{z_{13}}{z_9}$$

$$i_8 = \frac{z_{14}}{z_2} \cdot \frac{z_4}{z_{14}} \cdot \frac{z_{10}}{z_3} \cdot \frac{z_8}{z_{11}} \cdot \frac{z_{13}}{z_9}$$

The recorded ratios from i_1 to i_4 allow operation with gears from 1 to 4 forward. On the other hand, ratios from i_5 to i_8 allow operation with gears from 5 to 8 and the reverse gear.

The toothed gear z_3 can be separated from the toothed pairs in **Figure 2** and recordings of the gear ratios. The gear simultaneously creates kinematic pairs by engaging with the gears, z_1, z_5, z_{10}, which denotes that the toothed gear z_3 has an engagement frequency of 3. **Figure 1** shows an example of engagement frequency for the gear z_3, which is a driven gear with respect to gear z_1 and at the same time a follower gear with respect to gears z_5 and z_{10}.

CONTACT STRESSES AND SLIPPAGE WITHIN CHARACTERISTIC CONTACT POINTS

Contact stresses being a measure of the material effort used in durability calculations **[L. 5, 6, 9–13]** were determined at Point C being the pitch point located in the area of single-tooth engagement. The slippage were determined in three characteristic contact points: E_1 – the beginning of the active outline in area of double-tooth engagement, C – the pitch point, also called the rolling point of contact, E_2 – the end of the active outline in area of double-tooth engagement. Point E_2 can be placed on the tooth tip if the tooth has no bevel and in this case the diameter d_{E2} is equal to the diameter of the toothed gear heads, as shown in **Figure 3**.

At the Point E_1, determined by the diameter d_{E1}, there is the beginning of the active outline of the tooth in which area of double-tooth engagement also starts, ending at Point B_1 determined by diameter d_{B1}. At the same time, Point B_1 is the starting point of the single tooth engagement that ends at Point B_2, determined by the diameter d_{B2}. Between Points B_1 and B_2, there is a Point C called the rolling contact point or the pitch point, determined by the rolling diameter d_C. Point E_2 is the end point of the involute profile, which is also the end of the double-tooth engagement area within the tooth tip.

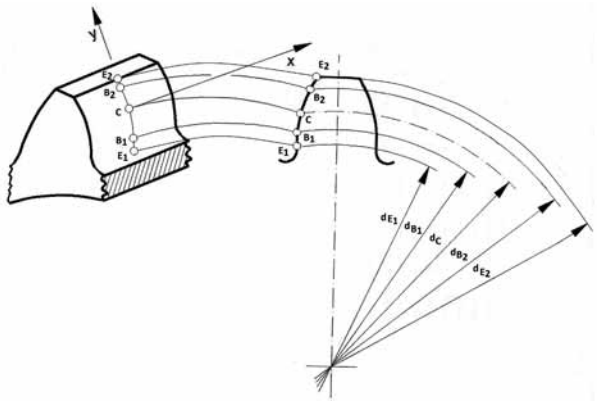

Fig. 3. Characteristic contact points on the tooth of the toothed gear

Rys. 3. Charakterystyczne punkty przyporu na zębie koła zębatego

Contact stresses and slippage in toothed pairs (z_1:z_3, z_3:z_5, z_3:z_{10}) at torque load M = 2100 Nm and rotational speed n = 1500 min^{-1} of the input shaft have been determined at actual parameters of the toothed gears forming the gearbox structure shown in **Figure 2**.

The calculated contact stresses were referred to fatigue contact durability σ_{Hlim} determined experimentally **[L. 7]**; the value of which, for AISI 8620 steel depending on the finishing technology, is chipped teeth σ_{Hlim} = 1492 MPa, and ground teeth σ_{Hlim} = 1459 MPa. In the presented diagrams of **Figures 4, 5**, and **6**, in the correct order for the toothed pairs (z_1:z_3, z_3:z_5, z_3:z_{10}), the results of calculated contact stresses were marked. Based on these figures, it can be stated that the fatigue contact durability is not fully utilized in the toothed pairs under consideration.

Figure 4 shows the location of contact stresses $sigma_{H1}$ of the toothed gear z_1 = 44 and $sigma_{H3}$ of the gear z_3 = 44 with P-0 correction of correction factors x_1 = -0.25, x_3 = +0.25, with respect to fatigue contact durability shlim_1 and shlim_2. The calculated contact stresses caused by the torque M = 2100 Nm transferred by the toothed pair z_1:z_3 do not use all the material capacity in terms of fatigue contact durability.

Contact stresses within the toothed pair z_3:z_5, in which the gear z_3 is the driving gear for the gear z_5 are shown in **Figure 5**.

The gear z_3 is also the driving gear for gear z_{10}, for which the contact stresses are shown in **Figure 6**.

The value of contact stresses in the toothed pair z_3:z_5 is $sigma_{H3}$ = 777 MPa for gear z_3, and $sigma_{H5}$ = 678 MPa for gear z_5, respectively. These values are small compared to the fatigue contact durability

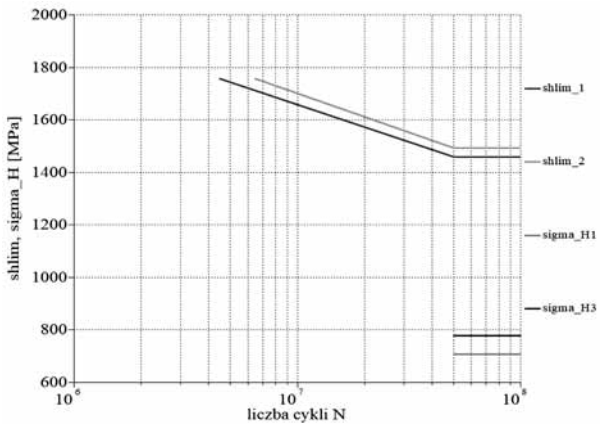

Fig. 4. Toothed pair z_1:z_3 with correction P-0 (x_1 = -0.25, x_3 = 0.25), $sigma_{H1}$ = 708 MPa, $sigma_{H3}$ = 777 MPa

Rys. 4. Para zębata z_1:z_3 z korekcją P-0 (x_1 = -0,25, x_3 = 0,25), $sigma_{H1}$ = 708 MPa, $sigma_{H3}$ = 777 MPa

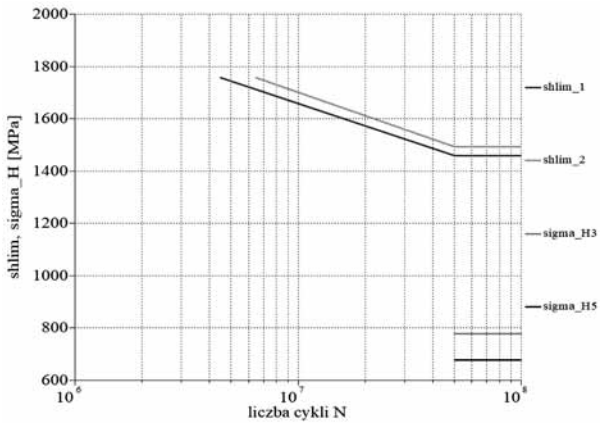

Fig. 5. Toothed pair z_3:z_5 with correction P-0 (x_3 = 0.25, x_5 = -0.25), $sigma_{H3}$ = 777 MPa, $sigma_{H5}$ = 678 MPa

Rys. 5. Para zębata z_3:z_5 z korekcją P-0 (x_3 = 0,25, x_5 = -0,25), $sigma_{H3}$ = 777 MPa, $sigma_{H5}$ = 678 MPa

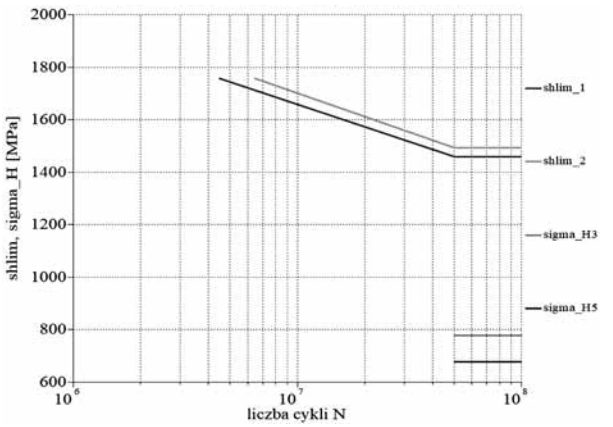

Fig. 6. Toothed pair z_3:z_{10} with correction P-0 (x_3 = 0.25, x_{10} = -0.25), $sigma_{H3}$ = 777 MPa, $sigma_{H10}$ = 817 MPa

Rys. 6. Para zębata z_3:z_{10} z korekcją P-0 (x_3 = 0,25, x_{10} = -0,25), $sigma_{H3}$ = 777 MPa, $sigma_{H10}$ = 817 MPa

σ_{Hlim} = 1492 MPa or 1459 MPa. In the toothed pair z_3:z_{10}, gear z_3 is subjected to contact stress of $sigma_{H3}$ = 777 MPa, and the gear z_{10} to stresses of $sigma_{H10}$ = 817 MPa. In all considered toothed pairs (z_1:z_3, z_3:z_5, z_3:z_{10}), contact stresses are much smaller than the fatigue contact durability σ_{Hlim}, which means that the considered toothed pairs do not have properly selected geometrical parameters for the given load.

In order to improve the use of fatigue contact durability, while maintaining the number of teeth of all gears in the tested gearbox, a multi-criterion optimization procedure was used in geometric and durability calculations **[L. 15, 16]**. The software uses 11 partial criteria. The varying values in multi-criterion optimization were modules, flank angles, and correction factors. Results from calculations of contact stresses for toothed pairs (z_1:z_3, z_3:z_5, z_3:z_{10}) after optimization are shown in **Figures 7, 8**, and **9**.

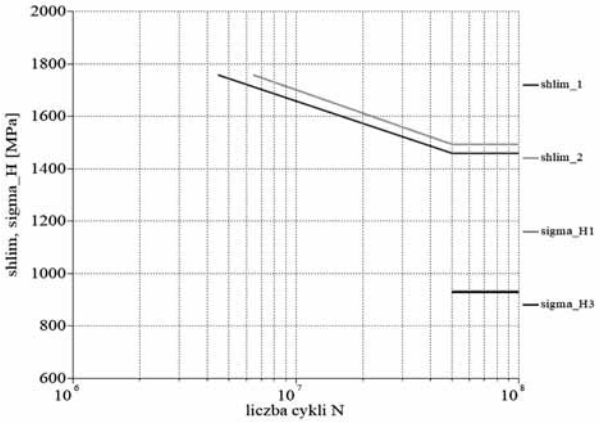

Fig. 7. Toothed pair z_1:z_3 with correction P after optimization

Rys. 7. Para zębata z_1:z_3 z korekcją P po optymalizacji

w

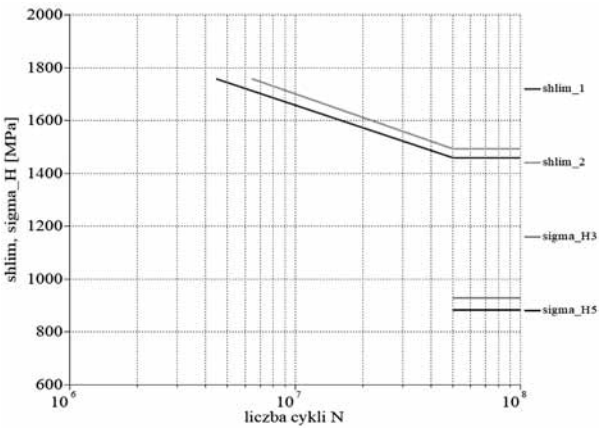

Fig. 8. Toothed pair z_3:z_5 with correction P after optimization

Rys. 8. Para zębata z_3:z_5 z korekcją P po optymalizacji

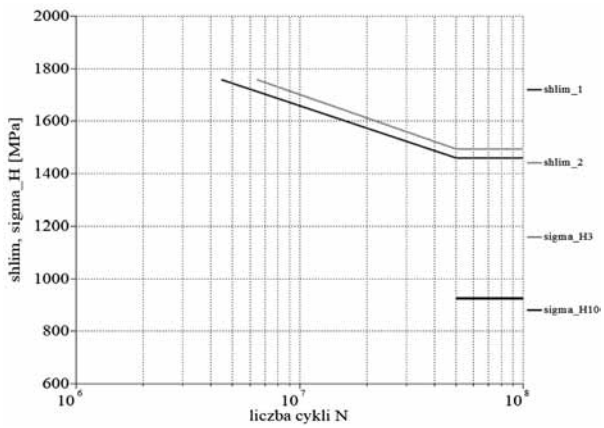

Fig. 9. Toothed pair z_3:z_{10} with correction P after optimization

Rys. 9. Para zębata z_3:z_{10} z korekcją P po optymalizacji

The multi-criterion optimization has reduced the difference between the calculated contact stresses and the stresses corresponding to fatigue contact durability. In spite of the optimization, maintaining gear ratios unchanged, the fatigue contact durability is still largely unused.

For toothed pairs, z_1:z_3, z_3:z_5, z_5:z_{10}, with correction P-0, slippage was determined at three contact points (E_1, C, E_2), and the values are graphically illustrated in **Figure 10**.

At Point E_1, which is the beginning of the active tooth outline, and at Point E_2 that ends the active tooth outline, the slippage values reach maximum (at E_1 in the tooth root there is a negative value, and at the E_2 point in the tooth tip there is a positive value). This is due to length of the involute curvature radius. In each case, at the Point C defined as the central contact point (or the pitch point), the slippage velocity equals zero.

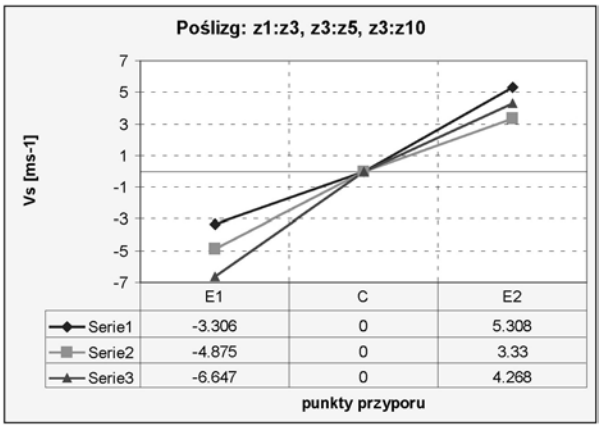

Fig. 10. Slippage in toothed pairs: z_1:z_3, z_3:z_5, z_5:z_{10} with correction P-0 (x_1 = -0.25, x_3 = 0.25, x_5 = -0.25, x_{10} = -0.25)

Rys. 10. Poślizgi w parach zębatych: z_1:z_3, z_3:z_5, z_5:z_{10} z korekcją P-0 (x_1 = -0,25, x_3 = 0,25, x_5 = -0,25, x_{10} = -0,25)

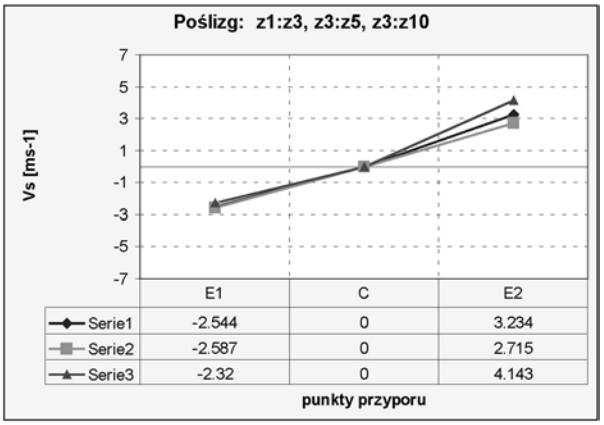

Fig. 11. Slippage in toothed pairs: z_1:z_3, z_3:z_5, z_5:z_{10} with correction P (x_1 = 0.0804, x_3 = 0.2059, x_5 = 0.2104, x_{10} = 0.6212)

Rys. 11. Poślizgi w parach zębatych: z_1:z_3, z_3:z_5, z_5:z_{10} z korekcją P (x_1 = 0.0804, x_3 = 0,2059, x_5 = 0,2104, x_{10} = 0,6212)

By introducing positive correction P in individual toothed pairs, slippage values and their differences are reduced, which is visible in **Figure 11**.

The comparison of slippage from **Figures 10** and **11** indicates how beneficial it is to use positive P correction. In addition to reducing the slippage value, the reduction of scatter is also visible in **Figure 11**.

ANALYSIS OF THE TEST RESULTS

In the conducted numerical tests with optimization on the 8-ratio power shift gearbox, the criterion of the assessment was contact stresses and slippage. The calculated values of contact stresses were referred to fatigue contact durability σ_{Hlim} for AISI 8620 steel, which is 1459 MPa for ground teeth and 1492 MPa for chipped teeth. Toothed pairs with P-0 correction display the greatest value of unutilized fatigue contact durability, and this especially concerns the toothed pair z_3:z_5, in which the smallest contact stresses occur at $sigma_{H3}$ = 777 MPa and $sigma_{H5}$ = 678 MPa.

After applying the P correction, there was an improvement within use of fatigue contact durability. On the example of a toothed pair z_3:z_5, after the optimization process with the correction factor x_3 = 0.2059 and x_5 = 0.2104 and with the module m = 4.7588 and the flank angle α_o = 25°, contact stresses are $sigma_{H3}$ = 929 MPa and $sigma_{H5}$ = 883 MPa. At the gear z_3, there was an increase in fatigue contact durability use by 19.5%, and at gear z_5, it increased by 30.2%. This article does not analyse the remaining toothed pairs that form a complete gearbox; however, in each of them, there are similar relationships in the use of fatigue contact durability.

Slippage for the same toothed pairs with P-0 correction has the highest value in pair z_3:z_{10} and

amounts to Vs_{3E1} = 6.647 m×s^{-1} and V_{s3E2} = 4.268 m×s^{-1}. After applying the P correction with coefficients x_3 = 0.2059 and x_{10} = 0.6212 and after optimization the slippage decreases, slippage reaches the values of Vs_{3E1} = 2.320 m×s^{-1} and V_{s3E2} = 4.143 m×s^{-1}. By introducing P correction and multi-criterion optimization, slippage values in each toothed pair decrease.

SUMMARY

Numerical studies with multi-criterion optimization enable selecting geometric properties of toothed gears in such a way to ensure the expected kinematic characteristics of the complete gearbox. In the analysed gearbox, the toothed gear z_3, due to tooth engagement equal to three, will be subject to the earliest wear by pitting. Hence, in this gear, greater contact durability is expected than it is in the case of the other gears. The use of P correction and multi-criterion optimization allows reducing differences in contact stresses and slippage in individual toothed pairs. Therefore, gearbox engineers should use positive correction P and multi-criterion optimization to utilize the known contact fatigue durability of a particular material to the maximum extent and to obtain the smallest possible value of slippage.

REFERENCES

1. Molari G., Sedoni E.: Experimental evaluation of power losses in a power shift agricultural tractor transmission. Biosystems Engineering 100 (2008).
2. Park S.M., Park T.W., Lee S.H., Han S.W., Kwon S.K.: Analytical study to estimate the performance of the power shift drive axle for a forklift. International Journal of Automotive Technology, vol. 11, 2010.
3. Tanelli M., Panzaui G., Savaresi S.M., Pirola C.: Transmission control for power shift agricultural tractors. Mechatronics, vol. 21, February 2011.
4. Pedrero J.I., Pleguezuelos M., Munoz M.: Contact stress calculation of undercut spur and helical gear teeth. Mechanism and Machine Theory, vol. 46, November 2011.
5. Li Ting, Pan Cunyun: On grinding manufacture technique and tooth contact and stress analysis of ring involute spherical gears. Mechanism and Machine Theory 44 (2009).
6. Pedrero J.I., Pleguezuelos M., Artes M., Antona J.A.: Load distribution model along the line of contact for involute external gears. Mechanism and Machine Theory, vol. 45, 2010.
7. Martyna M., Zwolak J.: Program komputerowy z optymalizacją wielokryterialną PRZEKŁADNIA. www.gearbox.com.pl.
8. Zwolak J.: System projektowania przekładni zębatych maszyn roboczych w ujęciu konstrukcyjno-materiałowo-technologicznym. Praca habilitacyjna. AGH Kraków, 2006.
9. Terrin A., Dengo C., Meneghetti G.: Experimental analysis of contact fatigue damage in case hardened gears for off highway axles. Engineering Failure Analysis 76 (2017).
10. Yegen I., Usta M.: The effect of salt bath cementation on mechanical behavior of hot-rolled and cold-drawn SAE 8620 and 16MnCr5 steels. Vacuum, vol. 85, 2010.
11. Osman T., Velex Ph.: A model for the simulation of the interactions between dynamic tooth loads and contact fatigue in spur gears. Tribology International, vol. 46, 2012.
12. Amarnath M., Sujatha C., Swarnamani S.: Experimental studies on the effects of reduction in gear tooth stiffness and lubricant film thickness in a spur geared system. Tribology International, vol. 42, 2009.
13. Sanchez M.B., Pedrero J.I., Pleguezuelos M.: Contact stress calculation of high transverse contact ratio spur and helical gear teeth. Mechanism and Machine Theory, vol. 64, June 2013.
14. Zwolak J., Martyna M.: The analysis of the slippage and contact stress in the meshing of the power shift type gear. Tribologia, nr 5, 2016.
15. Tarnowski W.: Optymalizacja i polioptymalizacja w technice. Wydawnictwo Uczelniane Politechniki Koszalińskiej, 2011.